Regular daily variations in satellite magnetic total intensity data

J. P. R. Turner, D. E. Winch, D. J. Ivers, R. J. Stening

Ann. Geophys., 25, 2167–2174, 2007
www.ann-geophys.net/25/2167/2007/

Annales Geophysicae

Regular daily variations in satellite magnetic total intensity data

J. P. R. Turner[1], **D. E. Winch**[1], **D. J. Ivers**[1], **and R. J. Stening**[2]

[1]School of Mathematics and Statistics, University of Sydney, Sydney, NSW 2006, Australia
[2]School of Physics, University of New South Wales, Sydney, NSW 2052, Australia

Received: 15 June 2007 – Accepted: 24 September 2007 – Published: 6 November 2007

Abstract. Regular magnetic daily quiet time (*Sq*) variations in total intensity of about 30 nT amplitude are determined in Universal Time (UT) from satellite magnetic field measurements. The CHAMP satellite traverses all hours of local time in 132 days and the *Sq* variations in total intensity are therefore calculated as an average over the 132 days for each hour of UT. Results are compared with the *Sq* daily variations in total intensity for the region above the ionosphere calculated from Malin's (1973) spherical harmonic analysis of the *Sq* Fourier coefficients for hourly mean value magnetic data from a global distribution of ground-based magnetic observatories. From the reasonable agreement between the two calculations, we conclude that low-Earth orbit satellites that traverse all hours of local time can determine *Sq* variations in total intensity above the ionosphere.

Keywords. Geomagnetism and paleomagnetism (Time variations, diurnal to secular) – Ionosphere (Mid-latitude ionosphere) – Magnetospheric physics (Current systems)

1 Introduction

All magnetic data, including satellite magnetic data, are a sum of magnetic fields from different sources. The principal sources are the slowly varying main field and the static lithospheric or crustal anomaly field. There are regular daily variation fields arising from electrical current systems in the ionosphere, magnetosphere and ocean. There are also magnetic fields from eddy currents induced in the ocean, the conducting Earth and the ionosphere by the various primary variation fields. The more rapidly changing fields include disturbance variation fields from magnetic storms. The regular daily variation consists of quiet day solar (*Sq*) and lunar (*L*) daily variations, and there is a disturbance daily variation field from the rotation of the Earth under a current system nearly symmetric about the geomagnetic dipole axis. The present study examines the quiet day solar daily variation *Sq* in satellite magnetic total intensity data.

Previous global studies of regular magnetic variations have mostly relied on ground based observatory data to provide global spherical harmonic mathematical representations of the daily variation fields. These representations are used for studies of the ionospheric dynamo, eigenmodes of atmospheric movement and electrical conductivity of the Earth's interior. Spherical harmonic analyses of the magnetic daily variations have been made on observatory data recorded during the Second International Polar Year 1933, the International Geophysical Years (IGY) July 1957 to December 1958 and the International Quiet Sun Years (IQSY) 1964–1965. Benkova (1940) analysed *Sq* during the International Polar Year of 1933. Parkinson (1971) analysed *Sq* for the International Geophysical Years (IGY), which were years of high sunspot number. Malin (1973) analysed solar and lunar magnetic variations for the IGY years. Winch (1981) analysed solar, lunar and lunar-elliptic tides and their seasonal change for the International Quiet Sun Years (IQSY) of 1964 and 1965.

The previous regular variation studies, which are all based on magnetic ground data, have limitations. The first is the poor global distribution of ground-based observatories, especially over the oceans and particularly in the Southern Hemisphere. The unevenness of the observatory distribution with longitude is not as important in local time studies as it is for studies in Universal Time (UT), because the magnetic daily variations depend very strongly on local time. However, problems with the uneven distribution in latitude remain. The poor distribution could be mitigated but only at considerable cost. The second limitation of the previous studies is that vector daily variations from ground-based observatories cannot distinguish between the external fields produced by electrical currents in the ionosphere and by electrical currents in

Correspondence to: D. E. Winch
(denisw@maths.usyd.edu.au)

Published by Copernicus Publications on behalf of the European Geosciences Union.

the magnetosphere, without additional modelling hypotheses concerning the variations of ionospheric and magnetospheric origin. This second limitation cannot be overcome by any measurements between the ground and the ionosphere.

Satellite magnetic field measurements can provide excellent global coverage, avoiding the uneven distribution of magnetic observatories. Daily variations determined from vector field measurements made at low Earth-orbit altitudes of about 400 km, above the ionosphere at 100 km altitude and below the magnetopause, should in principle be able to distinguish between the magnetic fields produced by currents in and below the ionosphere and by currents in the magnetosphere. This is analogous to the internal-external separation achieved with ground-based data. In this initial feasibility study of global *Sq* models in UT based on satellite data, we have used total intensity data, which provide excellent global coverage but do not allow separation of the magnetic field into internal and external parts.

Determination of global regular daily variations in UT from satellites in orbit before CHAMP has not been possible because of their limited local time coverage. A review of satellites used to measure the Earth's main magnetic field is given in Langel and Hinze (1998). The first satellite to survey the vector components of the Earth's magnetic field with high accuracy was the MAGSAT satellite, operational from 4 November 1979 to 11 June 1980. The MAGSAT satellite orbit was chosen so that it would remain close to the dawn-dusk terminator, and consequently, MAGSAT magnetic data were limited to the local times near dawn and dusk, (e.g. Langel et al., 1982). The Ørsted satellite of the Danish Meteorological Institute, launched on 23 February 1999, commenced orbit at 14:11 h local time, with its orbital plane drifting at -0.76 degrees per day. Thus, it took 237 days to move through 12 h of local time. By contrast, the satellite CHAMP, launched on 15 July 2001, has its orbital plane drifting at -1.36 degrees per day, and traverses all local times in 132 days. This allows the construction of global daily variation models in UT. These models can be interpreted as fields in UT, which have been averaged over 132 days. The orbital parameters of CHAMP were chosen specifically to enable separation of constituents of periodic phenomena such as tides and day-night variations at about 400 km altitude, well above the ionosphere and well below the magnetopause.

In this study we have used CHAMP total intensity data because of its quality and completeness globally and in local time and its almost circular orbit. In Sect. 2 the analysis used to determine the total intensity daily variation from the total intensity satellite magnetic data is described. In Sect. 3 it is shown to a good approximation that the variation in total intensity equals the component of the variation in the vector field in the direction of the main field. This result enables the use, in Sect. 4, of the *Sq* model of Malin (1973) to construct the total intensity daily variation field at the mean satellite altitude, under several modelling assumptions. The CHAMP satellite results are compared with the observatory based *Sq* model in Sect. 5. The use of vector satellite data is discussed in Sect. 6. Concluding remarks are made in Sect. 7.

Global studies of regular daily variations using ground-based observatory data exclude high latitude observatories to avoid any effects from the auroral zone current systems. Our principal interest here is also limited to equatorial and mid-latitude observatories, but our analysis of CHAMP satellite magnetic data has included the auroral regions. Both the northern and southern auroral zones show a significant regular daily change. We note that Ritter et al. (2004) in a study of ionospheric currents at auroral latitudes have made simultaneous estimates from the CHAMP satellite and a ground-based magnetometer network.

2 Analysis of the satellite magnetic data

In this study, the global form of the daily variation field in total intensity on quiet days is examined in UT, using CHAMP total intensity data for the period 15 May to 25 September 2001. The sampling period of the CHAMP scalar magnetometers is one second, so that there is a maximum of 84 600 records per day, although technical problems have reduced the actual amount of data available. The orbital plane drifts at -1.36 degrees per day, corresponding to -2.76 h of local time per standard month (of 365.24/12=30.44 days), and therefore a 12-h drift in local time will occur after 4.35 standard months (equal to 132 days) have elapsed.

In order to obtain the *Sq* variation for magnetically quiet days, only those data are chosen which have equivalent three-hourly Ik_p values less than or equal to 35. The K_p index of magnetic activity is given from low to high activity in the form 1−, 1, 1+, 2−, 2, 2+, 3−, 3, 3+, 4−, etc., and a simpler form called the Ik_p index is used for satellite magnetic data. The same values in the Ik_p index are 7, 10, 13, 17, 20, 23, 27, 30, 33, 37, so that the Ik_p value 35 is between K_p indices 3+ and 4−, meaning on the quiet side of the spectrum of activity. Thus Ik_p=10×K_p, but for +, add on 3, and for − subtract 3.

The satellite CHAMP has an orbital period of 93.5 min, and therefore during 4.35 standard months there are 2037 daytime equatorial crossings. The satellite also has a night-time crossing for each orbit, so that the total number of equatorial crossings regardless of each epoch, local time or UT, is 4073. The global picture for one hour of UT reduces the number of equatorial crossings to about 170. Thus when the data are gathered in bins of 1° of latitude by 1° of longitude, there is just one satellite track for every two equatorial bins. However, the distribution of bins with tracks is still much better than the distribution of ground-based observatories, for which there are huge gaps, such as the Great Southern Ocean.

In the analysis, all the observations for the 4.35 standard months were partitioned into 144 data sets corresponding to 10-min periods covering the entire UT day. Sets of selected data, each for one hour of UT and consisting of six 10-min data sets were extracted and then binned on a 1° latitude

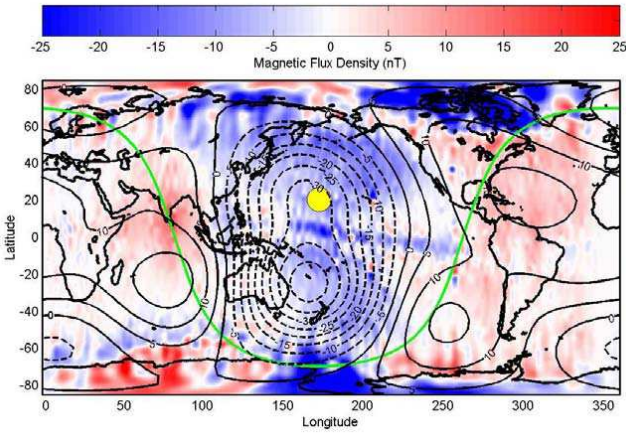

Fig. 1. *Sq* magnetic daily variation in CHAMP satellite total intensity magnetic data at 00:30 UT shown as a red-blue surface plot. The equivalent contours of the *Sq* total intensity field above the ionosphere, 00:30 UT, are calculated from spherical harmonic coefficients for IGY.

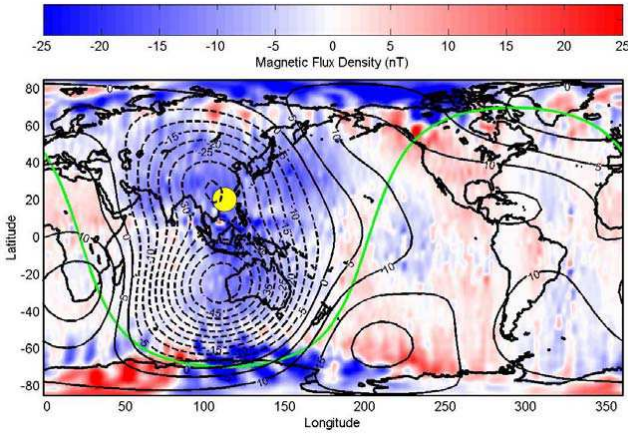

Fig. 2. *Sq* magnetic daily variation in CHAMP satellite total intensity magnetic data at 04:30 UT shown as a red-blue surface plot. The equivalent contours of the *Sq* total intensity field above the ionosphere, 04:30 UT, are calculated from spherical harmonic coefficients for IGY.

by 1° longitude grid. The binned data sets were then filtered using spatial pass filtering and notch filtering routines to remove low-level unwanted effects caused by bin-filling and "furrowing" along the satellite tracks. The method, and the selection of quiet days, is described in detail in Ivers et al. (2000). This produced 24 one-hour of UT global data sets.

The orbit of the CHAMP satellite is almost circular, but the variation in the main field over a small range of orbital altitude has a significant effect on the *Sq* field and must be removed. To remove the effect of the main field a suitable main field model must be subtracted. We chose the main field model of Olsen (2002) for epoch 2000. However, after the subtraction of the main field model, there remained a heavy zonal trend in the binned residues of the one-hour of UT global files. This zonal trend, which included the crustal anomaly field, masked the regular daily variation. Each one-hour of UT global file consists of data from different days, and therefore to remove the zonal trend, local midnight values were subtracted from the residue, the removal of daily means being impractical.

The local midnight values were obtained from the appropriate parts of the 24 one-hour UT data sets. From knowledge of the middle of the UT range of each dataset, the longitude at which local midnight occurs was determined. That subset of the dataset was then used to build a consolidated local midnight dataset. When completed, the consolidated local midnight dataset was subtracted from each of the primary datasets to give 24 corrected one hour UT data sets. When plotted, as in Figs. 1–6, these corrected data sets show a clear image of the regular magnetic daily variation and the local time dependence of the equatorial electrojet along the magnetic equator.

3 *Sq* daily variations in total intensity

Let $\boldsymbol{B}_{mf}$ be the magnetic flux density of Earth's main magnetic field, $\delta\boldsymbol{B}$is a small perturbation in $\boldsymbol{B}_{mf}$, T is the total intensity of the main field and δT is a small perturbation in T. Note that the field δT is not the magnitude of $\delta\boldsymbol{B}$, and can take both positive and negative values. Thus, $T^2{=}\boldsymbol{B}_{mf}{\cdot}\boldsymbol{B}_{mf}$ and $(T{+}\delta T)^2{=}(\boldsymbol{B}_{mf}{+}\delta\boldsymbol{B}){\cdot}(\boldsymbol{B}_{mf}{+}\delta\boldsymbol{B})$. Neglecting terms of second order in δT and $\delta\boldsymbol{B}$, we may write to first order

$$T^2 + 2T\,\delta T = \boldsymbol{B}_{mf}\cdot\boldsymbol{B}_{mf} + 2\boldsymbol{B}_{mf}\cdot\delta\boldsymbol{B},$$

which reduces to

$$T\,\delta T = \boldsymbol{B}_{mf}\cdot\delta\boldsymbol{B}.$$

Denoting the unit vector in the direction of the main magnetic field by $\widehat{\boldsymbol{B}}_{mf}{=}\boldsymbol{B}_{mf}\big/T$ and setting $\delta\boldsymbol{B}{=}\boldsymbol{B}_{Sq}$, the small change $\delta T{=}T_{Sq}$ in total intensity Tcaused by the presence of the regular daily variation field *Sq* is

$$T_{Sq} = \widehat{\boldsymbol{B}}_{mf}\cdot\boldsymbol{B}_{Sq} \quad . \tag{1}$$

Therefore, the regular daily variation in total intensity T_{Sq} is the component of the regular daily variation vector field in the direction of the Earth's main magnetic field. Near the magnetic poles T_{Sq} is predominantly the vertical component of the vector regular daily variation, and near the magnetic equator it is mainly the northward component. The neglect of the higher order terms is justified, since $\delta T\big/T$approximately equals $|\delta\boldsymbol{B}|\big/\big|\boldsymbol{B}_{mf}\big|{\sim}10^{-3}$.

4 $\boldsymbol{B}_{Sq}$ at satellite altitude from observatory data

The regular daily variation in total intensity T_{Sq} can be determined using Eq. (1) from models for *Sq* and the main field

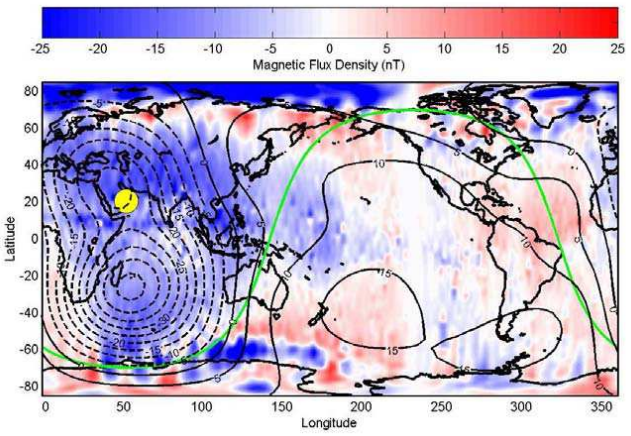

Fig. 3. *Sq* magnetic daily variation in CHAMP satellite total intensity magnetic data at 08:30 UT shown as a red-blue surface plot. The equivalent contours of the *Sq* total intensity field above the ionosphere, 08:30 UT, are calculated from spherical harmonic coefficients for IGY.

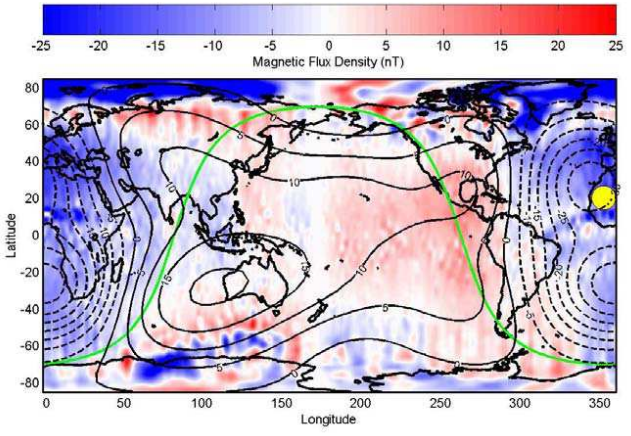

Fig. 4. *Sq* magnetic daily variation in CHAMP satellite total intensity magnetic data at 12:30 UT shown as a red-blue surface plot. The equivalent contours of the *Sq* total intensity field above the ionosphere, 12:30 UT, are calculated from spherical harmonic coefficients for IGY.

at the same epoch. The analyses of Malin (1973) for the IGY years of relatively high sunspot number and of Winch (1981) for the IQSY years of relatively low sunspot number are the only analyses available for comparison with the CHAMP results, and both were for epochs well before that of CHAMP. To compare the CHAMP satellite results with an *Sq* model derived from observatory data of a different epoch, a similar level of solar activity is required. The average sunspot number was 114 for the interval from 15 May 2001 to 25 September 2001 over which the CHAMP data were analysed.

The average sunspot number was 187 for the interval from 1 July 1957 to 31 December 1959 over which Malin (1973) analysed IGY data and for the IQSY years 1964 and 1965, the sunspot number was much smaller, at 15. For this reason, the Malin (1973) *Sq* variation coefficients for the IGY were considered more suitable for the present purpose of comparison than those of Winch (1981) for the IQSY years. For the main field in Eq. (1), and using Malin's *Sq* results, the IGRF 1955 was used.

In the analysis of observatory magnetic data, Fourier analyses of hourly mean values for magnetic field components provides sets a and b Fourier coefficients, and these are then subjected to spherical harmonic analysis in the usual way, so as to separate the field into internal and external parts. For satellite magnetic data, the situation is rather different. Global distributions of values of field components are obtained at a fixed UT, then the main field and midnight values are removed to give a global distribution of values. In the present case, a global distribution of *Sq* total intensity values is derived. Because we consider only global distributions at a fixed UT, the theory is presented as if it were a simple spherical harmonic analysis, and the particular hour of UT is left understood.

The main field unit vectors in Eq. (1) were computed at all points on a 1° latitude by 1° longitude grid at the mean satellite altitude. These computations are standard and need not be described. However, the evaluation of the regular daily variation $\boldsymbol{B}_{Sq}$ in Eq. (1) at the mean satellite altitude, i.e. above the ionosphere, using Malin's (1973) model is more subtle, since the *Sq* model was derived from observatory data for the region between the Earth's surface and the ionosphere. This region will be referred to as region B and the region between the ionosphere and the magnetopause will be called region A. Region B has constant magnetic permeability and is a poor electrical conductor. Thus, the current density in region B is effectively zero and the magnetic field flux density $\boldsymbol{B}_{Sq}$ of the regular daily magnetic variations is the gradient of a scalar potential V_{Sq}, i.e., $\boldsymbol{B}_{Sq}=-\nabla V_{Sq}$. Since $\nabla\cdot\boldsymbol{B}_{Sq}=0$, it follows that the potential function V_{Sq} of the magnetic regular daily variations in the region between the Earth and the ionosphere, satisfies Laplace's equation, i.e.

$$\nabla^2 V_{Sq} = 0.$$

The general solution for V_{Sq} in a spherical polar coordinate system (r, θ, ϕ), where r is the spherical radius, θ is the geocentric colatitude and ϕ is the east longitude, can be written as

$$V_{Sq}(r,\theta,\phi) = a\sum_{n=1}^{N}\sum_{m=0}^{n}\left(\tfrac{a}{r}\right)^{n+1}(g_{ni}^{m}\cos m\phi + h_{ni}^{m}\sin m\phi)P_n^m(\cos\theta) + a\sum_{n=1}^{N}\sum_{m=0}^{n}\left(\tfrac{r}{a}\right)^{n}(g_{ne}^{m}\cos m\phi + h_{ne}^{m}\sin m\phi)P_n^m(\cos\theta)\ .$$

The parameter a represents the radius of a reference sphere, usually taken as the mean radius of the Earth. The leading

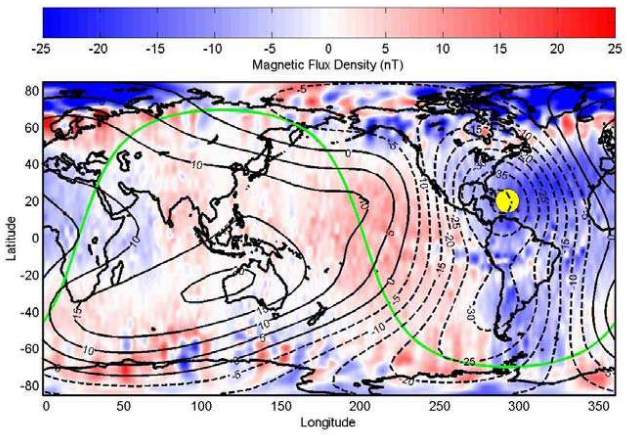

Fig. 5. *Sq* magnetic daily variation in CHAMP satellite total intensity magnetic data at 16:30 UT shown as a red-blue surface plot. The equivalent contours of the *Sq* total intensity field above the ionosphere, 16:30 UT, are calculated from spherical harmonic coefficients for IGY.

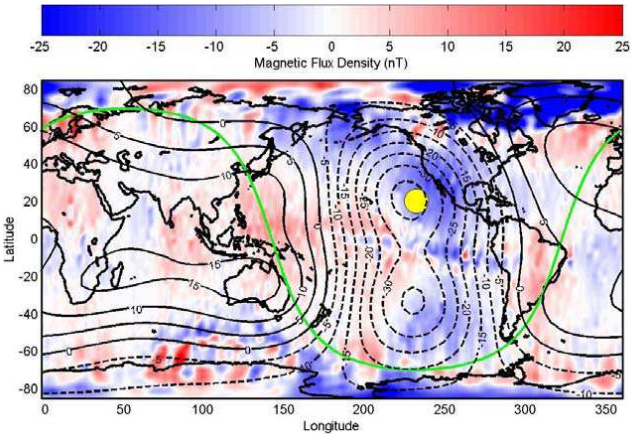

Fig. 6. *Sq* magnetic daily variation in CHAMP satellite total intensity magnetic data at 20:30 UT shown as a red-blue surface plot. The equivalent contours of the *Sq* total intensity field above the ionosphere, 20:30 UT, are calculated from spherical harmonic coefficients for IGY.

factor a is included so that the units of the g and h coefficients are those of magnetic flux density. For studies of the regular magnetic variations, using only terms of degree $N=8$ or less, the Earth's oblateness is ignored.

The potential function V_{Sq} consists of two distinct sums. The first sum contains descending powers of r and is produced by currents in the ionosphere and magnetosphere, i.e. currents "external" to region B. The second sum, which consists of ascending powers of r, arises from currents induced in the electrically conducting Earth and deep oceans by the overhead currents, and also currents arising from the dynamo action of tidal ebb and flow in the deep oceans, i.e. currents "internal" to region B.

The magnetic field elements of the regular daily variation, X_{Sq}, Y_{Sq}, Z_{Sq}, are given in spherical polar coordinates by

$$X_{Sq} = \frac{1}{r}\frac{\partial V_{Sq}}{\partial \theta}, Y_{Sq} = -\frac{1}{r\sin\theta}\frac{\partial V_{Sq}}{\partial \phi}, Z_{Sq} = \frac{\partial V_{Sq}}{\partial r}.$$

Thus, at $r=a$,

$$\begin{aligned}
X_{Sq} &= \sum_{n=1}^{N}\sum_{m=0}^{n}\left[(g_{ni}^m + g_{ne}^m)\cos m\phi\right. \\
&\quad \left.+(h_{ni}^m + h_{ne}^m)\sin m\phi\right]\frac{dP_n^m}{d\theta}, \\
Y_{Sq} &= \frac{1}{\sin\theta}\sum_{n=1}^{N}\sum_{m=0}^{n}\left[m(g_{ni}^m + g_{ne}^m)\sin m\phi\right. \\
&\quad \left.-m(h_{ni}^m + h_{ne}^m)\cos m\phi\right] P_n^m, \\
Z_{Sq} &= \sum_{n=1}^{N}\sum_{m=0}^{n}\left\{\left[-(n+1)g_{ni}^m + n\,g_{ne}^m\right]\cos m\phi\right. \\
&\quad \left.+\left[-(n+1)h_{ni}^m + n\,h_{ne}^m\right]\right\} P_n^m(\cos\theta).
\end{aligned}$$

The process of separation of the field (over a sphere of radius a, corresponding to the Earth) into internal and external coefficients is done in a single calculation using these representations for X_{Sq}, Y_{Sq}, Z_{Sq}.

The spherical harmonic coefficients g_{ni}^m, h_{ni}^m, g_{ne}^m, h_{ne}^m of the regular magnetic daily variations all depend on time. The dependence is strongly, but not entirely, on local time. Malin (1973) gave Fourier coefficients in time for both solar and lunar magnetic tides for the coefficients g_{ni}^m, h_{ni}^m, g_{ne}^m, h_{ne}^m at 1, 2, 3, and 4 cycles per day. From Malin's (1973) model the coefficients g_{ne}^m and h_{ne}^m and hence the 'external potential field' itself can be calculated at any UT in the region between the Earth's surface and the ionosphere.

Several hypotheses are required to extend Malin's (1973) model to the region between the ionosphere and the magnetopause. We have used four hypotheses:

(H1) the ionosphere is a thin spherical layer of radius R, which can be modelled by a spherical surface current;

(H2) the quiet day regular daily variation field of magnetospheric origin is much smaller than the quiet day regular daily variation field of ionospheric origin;

(H3) the quiet day regular daily variation field produced by electrical currents induced in the solid earth and oceans is negligible compared to the ionospheric quiet day regular daily variation field at the satellite altitude.

(H4) the non-potential part of the quiet day regular daily variation field is much smaller than the quiet day regular daily variation field of ionospheric origin.

The hypotheses are reasonable as a first approximation given the closeness of the satellite orbit to the ionosphere.

Denoting the potential in region B (between the Earth and the ionosphere) by $V_{Sq}^B(r,\theta,\phi)$, it follows from hypothesis (H3) that, relative to a sphere a radius R,

$$V_{Sq}^B(r,\theta,\phi) = R\sum_{n=1}^{N}\sum_{m=0}^{n}\left(\frac{r}{R}\right)^n (e_n^m\cos m\phi + f_n^m\sin m\phi)P_n^m(\cos\theta).$$

This potential must equal the external part of Malin's (1973) potential. Thus the coefficients e_n^m, f_n^m, can be derived from

the coefficients for the external field g_{ne}^m, h_{ne}^m, respectively, and

$$a\left(\frac{r}{a}\right)^n g_{ne}^m = R\left(\frac{r}{R}\right)^n e_n^m, a\left(\frac{r}{a}\right)^n h_{ne}^m = R\left(\frac{r}{R}\right)^n f_n^m.$$

Therefore, coefficients e_n^m and f_n^m are given by

$$e_n^m = \left(\frac{R}{a}\right)^{n-1} g_{ne}^m,\ f_n^m = \left(\frac{R}{a}\right)^{n-1} h_{ne}^m. \tag{2}$$

In region A, above the ionosphere, $\boldsymbol{B}_{Sq}^A = -\nabla V_{Sq}^2 + \boldsymbol{B}_{Sq}^{np}$, where $\boldsymbol{B}_{Sq}^{np}$ is the non-potential part of the field $\boldsymbol{B}_{Sq}^A$, and where V_{Sq}^2 denotes the potential in region A. We neglect the non-potential field $\boldsymbol{B}_{Sq}^{np}$ by hypothesis (H4), and by (H2) there are no ascending powers of r in V_{Sq}^A. Thus $\boldsymbol{B}_{Sq}^A = -\nabla V_{Sq}^A$, where

$$V_{Sq}^A(r,\theta,\phi) = R\sum_{n=1}^{N}\sum_{m=0}^{n}\left(\frac{R}{r}\right)^{n+1} (I_n^m \cos m\phi + J_n^m \sin m\phi) P_n^m(\cos\theta)\ . \tag{3}$$

It is a condition derived from the equation, $\nabla\cdot\boldsymbol{B}=0$, that the normal component of magnetic flux density is continuous across any surface. This condition also holds for the quiet day regular daily variation field across the ionospheric current surface. Hypothesis (H1) is invoked at this point. Since the magnetic flux densities in regions A and B are given by $\boldsymbol{B}_{Sq}^A = -\nabla V_{Sq}^A$ and $\boldsymbol{B}_{Sq}^B = -\nabla V_{Sq}^B$, on the inside of the spherical surface $r=R$, the magnetic flux density is

$$\begin{aligned}\boldsymbol{B}_{Sq}^B(r,\theta,\phi)\Big|_{r=R} = -\sum_{n=1}^{N}\sum_{m=0}^{n} &\big[n(e_n^m\cos m\phi + f_n^m \sin m\phi) P_n^m(\cos\theta)\boldsymbol{e}_r \\ &+(e_n^m\cos m\phi + f_n^m\sin m\phi)\tfrac{dP_n^m}{d\theta}\boldsymbol{e}_\theta \\ &-\tfrac{m}{\sin\theta}(e_n^m\sin m\phi - f_n^m\cos m\phi)P_n^m(\cos\theta)\boldsymbol{e}_\phi\big],\end{aligned}$$

where $(\boldsymbol{e}_r, \boldsymbol{e}_\theta, \boldsymbol{e}_\phi)$ are the unit vectors in the spherical polar coordinates, and on the outside of the spherical surface $r=R$, the magnetic flux density is

$$\begin{aligned}\boldsymbol{B}_{Sq}^A(r,\theta,\phi)\Big|_{r=R} = -\sum_{n=1}^{N}\sum_{m=0}^{n} &\big[-(n+1)(I_n^m\cos m\phi + J_n^m\sin m\phi)P_n^m(\cos\theta)\boldsymbol{e}_r \\ &+(I_n^m\cos m\phi + J_n^m\sin m\phi)\tfrac{dP_n^m}{d\theta}\boldsymbol{e}_\theta \\ &-m(I_n^m\sin m\phi - J_n^m\cos m\phi)P_n^m(\cos\theta)\boldsymbol{e}_\phi\big].\end{aligned} \tag{4}$$

From the radial components of $\boldsymbol{B}_{Sq}^A$ and $\boldsymbol{B}_{Sq}^B$, it follows that the coefficients e_n^m, f_n^m, for the interior and I_n^m, J_n^m, for the exterior, are related by

$$n\,e_n^m = -(n+1)I_n^m,\ n\,f_n^m = -(n+1)J_n^m. \tag{5}$$

Combining Eqs. (2) and (5), the potential field (Eq. 3) above the ionospheric current system has coefficients I_n^m, J_n^m, which can be expressed in terms of external field coefficients from the analysis of observatory based data,

$$\begin{aligned} I_n^m &= -\tfrac{n}{n+1}e_n^m = -\tfrac{n}{n+1}\left(\tfrac{R}{a}\right)^{n-1} g_{ne}^m, \\ J_n^m &= -\tfrac{n}{n+1}f_n^m = -\tfrac{n}{n+1}\left(\tfrac{R}{a}\right)^{n-1} h_{ne}^m. \end{aligned} \tag{6}$$

It can be seen from these formulae that the effect of low degree harmonics is greatly reduced on the outside of the spherical current sheet. When $n=1$, for example, a factor $1/2$ is applied to the external field coefficients g_{ne}^m and h_{ne}^m determined from observatory data.

The total intensity field, $T_{Sq} = \left|\boldsymbol{B}_{Sq}^A(R,\theta,\phi)\right|$, is constructed from Eqs. (4) and (6). The level contours of T_{Sq} are plotted in contour form in Figs. 1 to 6. The contours show negative values during daylight hours and weaker positive values during nighttime hours.

5 Results

Results from the analysis of CHAMP data at each epoch of local time are based on an average of results from satellite tracks over 132 days. The results for the regular daily variation are given, in colour, at four-hourly intervals of UT, in Figs. 1 to 6. These figures also show the position of the Sun (the yellow disk) and the location of the dawn-dusk terminator (the line between day and night). Blue is used for negative values, and red for positive values according to the scale given. Note that the CHAMP results do not distinguish between fields of internal and external origin. The CHAMP data include data from the June solstice but not from the December solstice, so that the CHAMP magnetic data for the 132 days are weighted to the northern summer. This explains the greater local time extent of negative (blue) values in the Northern Hemisphere in Figs. 1 to 6.

For the purpose of comparison, the results from the Malin (1973) analysis of observatory Fourier coefficients are overlaid as contours in Figs. 1 to 6. There are obvious similarities between the results from the analysis of the CHAMP data and those calculated from the Malin (1973) coefficients for the external *Sq* field. The overlaid contours are not those of an equivalent current system, but represent values calculated for the regular daily variation of total intensity T at each point of a 1° by 1° grid, at each UT indicated, from independent data sets for each figure. Both sets of figures have a sectorial appearance, with negative values, corresponding to a reduction in total intensity of the field, occurring in almost the entire sunlit hemisphere. Surrounding the strong daylight negative (blue) values is a boundary of positive (red) values, with the 10 or 20 nT contour lines that tend to follow the terminator, especially the morning terminator, in a number of the diagrams. The nighttime contours show mainly positive (red) values, with diffuse maxima, some of up to 25 nT. The auroral zones show daily variation terms that do not appear

in the Malin (1973) results, because high latitude observatories were excluded from the Malin (1973) spherical harmonic analysis.

The overlaid contours in Figs. 1 to 6 show negative values with minima of -50 nT appearing in the daylight hemisphere, with a small east-west 'saddle' above the equatorial electrojet and between the minima that form on the northern and southern sides of the magnetic equator. The magnetic fields arising from the current system in the sunlit hemisphere act to oppose the main field, and therefore appear as blue values in Figs. 1 to 6. There are also, typically, current function contours in the nighttime hemisphere. The nighttime current system is unlikely to be ionospheric, and more likely to be of magnetospheric origin.

The total intensity daily variations in CHAMP satellite data show daytime minima of about 25 nT, and also show the equatorial electrojet along the dip equator. In particular, it can be seen that the equatorial electrojet forms in the morning hours after sunrise, and, exists from the pre-noon hours until sunset. See Ivers et al. (2003) and Lühr et al. (2004).

Making some allowance for the differences in sunspot number for the two chosen epochs, as well as underlying assumptions, the agreement between the results of analysis of the CHAMP data, and the analysis of the potential fields used by Malin (1973), is quite good. As expected from the sunspot number ratio 187 to 114, for the Malin (1973) and CHAMP data epochs respectively, the Malin (1973) analysis minima are greater than the corresponding minima from the CHAMP data.

6 Discussion

There are new features in satellite magnetic data not present in ground-based data. The magnetic field determined from vector field measurements on a spherical surface in an electrically insulating region, such as the Earth's surface, can be separated into an internal component produced by the current interior to the surface and an external component produced by the current exterior to the surface. In the current-free region analysis of the magnetic field $\boldsymbol{B}$ is simplified by the existence of a harmonic magnetic scalar potential V, so that $\boldsymbol{B}=-\nabla V$ with $\nabla^2 V=0$. Improvements can be made to account for the oblateness of the Earth's surface but to still allow the separation of the magnetic field into fields of internal and external origin.

Satellite measurements, however, are made in a region containing electrical currents, where in general, the magnetic field $\boldsymbol{B}$ is not the gradient of a scalar potential. But the magnetic field can be represented everywhere, even in a conducting region, as the sum of toroidal and poloidal fields,

$$\boldsymbol{B} = \nabla \times T\boldsymbol{r} + \nabla \times \nabla \times S\boldsymbol{r},$$

where $\boldsymbol{r}$ is the radius vector from some chosen origin. The poloidal magnetic field on any spherical surface concentric with the origin is a sum of an internal part, which arises from the toroidal current inside the surface, and an external part, which arises from the toroidal current outside the surface. The toroidal magnetic field on the surface arises from the radial current at the surface. Thus the vector magnetic field on a spherical surface concentric with the origin is a sum of three fields: an internal poloidal magnetic field, an external poloidal magnetic field and a toroidal magnetic field. The internal part determined at satellite altitudes is from ionospheric currents and from currents induced in the solid Earth and oceans; the external part is that produced by the currents in the magnetosphere. Of course, satellite magnetic data cannot distinguish between magnetic fields of ionospheric origin and the main magnetic field, as is routinely done with observatory magnetic data. The toroidal field is often referred to as the non-potential field, however this terminology can be misleading, since the internal and external poloidal parts may also be non-potential fields. There is no way to determine if the poloidal part is non-potential from knowledge of only the vector magnetic field on the spherical surface.

In some ground-based main field studies, a non-potential toroidal field has been assumed, which arises from electric currents, often termed "Earth-to-air" currents. However, there is no toroidal component and, more generally, no non-potential component present in magnetic field measurements made at ground level, because a non-zero non-potential magnetic field cannot exist in the non-conducting region below the ionosphere. Thus the non-potential field in the ionosphere and above, and its currents, cannot be determined from the analysis of ground-based magnetic data.

Analysis of satellite magnetic data is further complicated by the fact that satellite orbits do not usually lie on a surface but traverse a shell-like region. The radial dependence of the toroidal-poloidal potentials, T and S, is then required to reduce the data to a mean spherical surface. For example, hypotheses for the choice of radial dependence of the toroidal field can be made which allow its interpretation in terms of a field-aligned current, e.g. Winch et al. (2005). Alternatively, approximations must be made. In this study two approximations have been used: the first is the neglect of the non-potential field, except perhaps in the ionosphere which is modelled as a spherical surface current; and the second is the assumption that the satellite orbit lies on a spherical surface. The first approximation, which is used in satellite main field studies, was employed in Sect. 4 to extend Malin's (1973) model above the ionosphere. The second approximation was used in the analysis of the CHAMP total intensity data.

The CHAMP data almost certainly include a magnetic field component due to electrical currents that cannot be represented by a scalar potential.

This non-potential field cannot be isolated using CHAMP total intensity field data and does not (and could not) appear in the results of the Malin (1973) analysis, because the atmosphere at altitudes below the ionosphere is an electrical insulator, and the required electrical currents (with a radial

component) cannot flow there. The identification of the non-potential field will rely on future analysis of CHAMP vector data.

7 Conclusions

With the exception of equatorial electrojet studies, all previous *Sq* analyses have been based on data recorded below the ionosphere at ground-based magnetic observatories. This present analysis has shown that magnetic daily variations in total intensity can be determined using magnetic data from satellites in low Earth orbit above the ionosphere. The results are in good agreement with magnetic variations derived from the equivalent electrical current system corresponding to the external field of magnetic daily variations determined from ground based magnetic observatory data. The results imply that analyses of vector daily variation fields above the ionosphere are possible, with the prospect of definitive results for daily variations in the separation of the magnetic field into parts originating above or below satellite low-Earth orbit levels, and the direct determination of daily variations of non-potential fields from current systems in the ionosphere-magnetopause region.

The same technique should allow the determination of the lunar variations *L* from satellite data.

Acknowledgements. Topical Editor M. Pinnock thanks S. Malin and another anonymous referee for their help in evaluating this paper.

References

Benkova, N. P.: Spherical harmonic analysis of the *Sq* variations, May–August 1933, Terr. Magn. Atmos. Elect., 45, 425–432, 1940.

Ivers, D. J., Stening, R. J., Turner, J. P. R., and Winch, D. E.: Ørsted and Magsat scalar anomaly fields, Earth Planets Space, 52, 1213–1225, 2000.

Ivers, D., Stening, R., Turner, J., and Winch, D.: Equatorial electrojet from Ørsted scalar magnetic field observations, J. Geophys. Res.-Space Phys., 108(A2), 1061, doi:10.1029/2002JA009310, 2003.

Langel, R. A., Ousley, G., Berbert, J., Murphy, J., and Settle, M.: The Magsat Mission, Geophys. Res. Lett., 9, 243–245, 1982.

Langel, R. A. and Hinze, W. J.: The magnetic field of the Earth's Lithosphere, Cambridge University Press, 46–49, 1998.

Lühr, H., Maus, S., and Rother, M.: Noon-time equatorial electrojet: its spatial features as determined by the CHAMP satellite, J. Geophys. Res., 109, A01306, doi:10.1029/2002JA009656, 2004.

Malin, S. R. C.: Worldwide distribution of geomagnetic tides, Phil. Trans. R. Soc. Lond., 274A, 551–594, 1973.

Olsen, N.: A model of the geomagnetic field and its secular variation for epoch 2000 estimated from Ørsted data, Geophys. J. Int., 149, 454–462, 2002.

Parkinson, W. D.: An analysis of the geomagnetic diurnal variation during the International Geophysical Year, Beiträge Geophys., 80, 199–232, 1971.

Ritter, P., Lühr, H., Viljanen, A., Amm, O., Pulkinnen, A., and Sillanpää, L.: Ionospheric currents estimated simultaneously from CHAMP satellite and IMAGE ground-based magnetic field measurements: a statistical study at auroral latitudes, Ann. Geophys., 22, 417–430, 2004, http://www.ann-geophys.net/22/417/2004/.

Winch, D. E.: Spherical harmonic analysis of geomagnetic tides, 1964–1965, Phil. Trans. R. Soc. Lond., 303A, 1–104, 1981.

Winch, D. E., Ivers, D. J., Turner, J. P. R., and Stening, R. J.: Geomagnetism and Schmidt quasi-normalization, Geophys. J. Int., 160, 487–504, 2005.